Impact of different nanoparticles on the thermal degradation kinetics of phenolic resin nanocomposites

L. Asaro, D. A. D'Amico, V. A. Alvarez, E. S. Rodriguez & L. B. Manfredi

Journal of Thermal Analysis and Calorimetry
An International Forum for Thermal Studies

ISSN 1388-6150

J Therm Anal Calorim
DOI 10.1007/s10973-017-6103-0

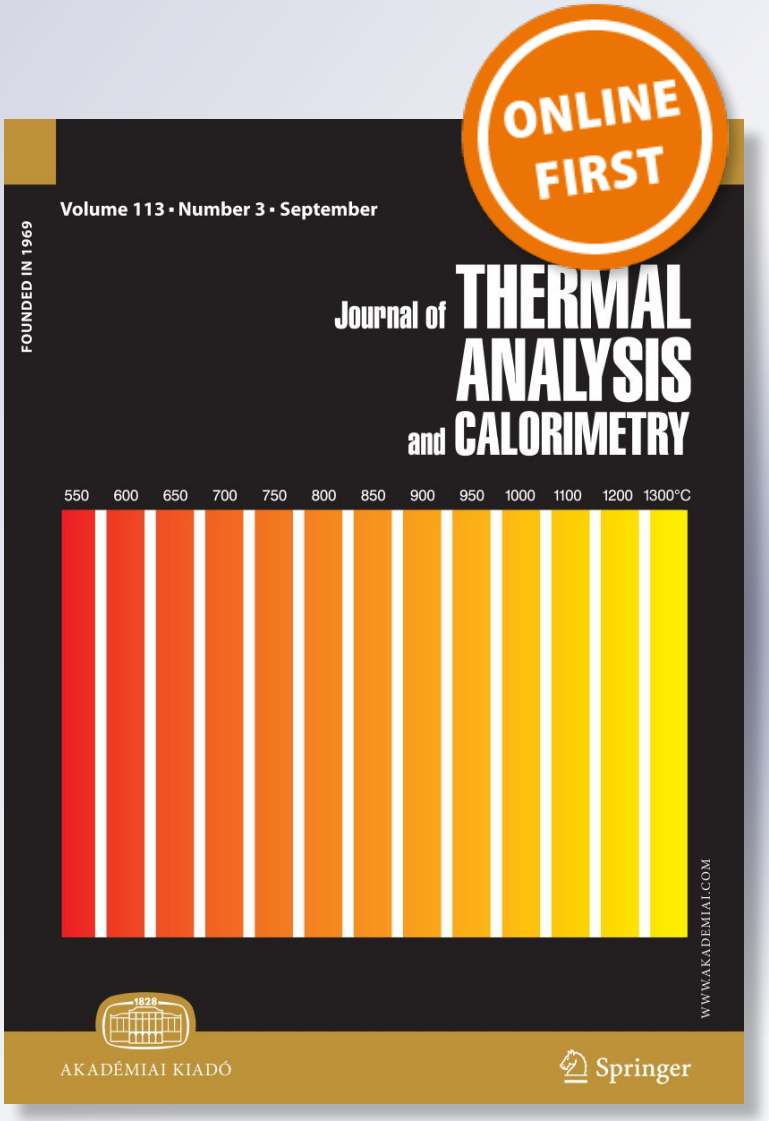

Springer

J Therm Anal Calorim
DOI 10.1007/s10973-017-6103-0

Impact of different nanoparticles on the thermal degradation kinetics of phenolic resin nanocomposites

L. Asaro[1] · D. A. D'Amico[2] · V. A. Alvarez[3] · E. S. Rodriguez[1] · L. B. Manfredi[2]

Received: 25 September 2016 / Accepted: 13 January 2017

Abstract The effect of different contents of nano-fillers: carbon black (CB), bentonites [original (Bent) and modified with phosphonium salt (B-TBHP)] and commercial modified montmorillonite (C30B) on the thermal degradation of phenolic resin was studied by thermogravimetric analysis (TG). The obtained results strongly suggest that CB was the most effective filler in improving the thermal stability of the resol-type phenolic matrix. The previous results were associated with the thermal stability of each filler but also with the compatibility between the matrix and the filler and the effect of filler incorporation on the cross-linking degree of the neat matrix. The profile of the apparent activation energy with the conversion of the thermal degradation process for the resol and the nanocomposites was obtained using three isoconversional methods: Friedman, KAS and Vyazovkin. The curves were correlated with the degradation steps of the phenolic resin observed by TG, showing a similar degradation mechanism for all the systems. By means of the method of invariant kinetic parameters, it was possible to estimate the preexponential factor and the activation energy to describe the degradation process of the resol and the nanocomposites in the thermal fragmentation zone, between 350 and 600 °C. It was determined that the Sestak–Berggren model was the one that best describes the thermal degradation experimental data. Then, a comparison between the experimentally obtained and the simulated differential degradation curves shows that the resulting model was certainly accurate to predict the thermal degradation process of the resol and the nanocomposites.

Keywords Phenolic resin · Nano-filler · Composites · Thermal degradation · Kinetic models

Introduction

Phenolic resins are among the first thermosetting resins synthesized and are still one of the most used in several applications such as matrix of high performance composite materials, coatings and adhesives. They are widely used due to their high flame resistance in addition to their excellent thermal and chemical stability [1].

Numerous studies have shown that the incorporation of nano-fillers, such as layered silicate clays, into polymers often improves their mechanical, thermal, barrier and physicochemical properties when compared with either the pure polymer or their conventional microcomposites, even at a very low filler concentration which leads to the nano-level interactions with the polymer matrix [2–10]. Furthermore, improvement of the physical properties of the final product of the nanocomposites is strongly dependent on the clay mineral–polymer compatibility, as well as on processing conditions. Two different morphological structures are

✉ L. B. Manfredi
lbmanfre@fi.mdp.edu.ar

[1] División Materiales Compuestos Estructurales Termorrígidos, Instituto de Investigaciones en Ciencia y Tecnología de Materiales (INTEMA), UNMdP, CONICET, Facultad de Ingeniería, Solís 7575, B7608FDQ Mar del Plata, Argentina

[2] División Ecomateriales, Instituto de Investigaciones en Ciencia y Tecnología de Materiales (INTEMA), UNMdP, CONICET, Facultad de Ingeniería, Av. Juan B Justo 4302, B7608FDQ Mar del Plata, Argentina

[3] División Materiales Compuestos de Matriz Termoplástica, Instituto de Investigaciones en Ciencia y Tecnología de Materiales (INTEMA), UNMdP, CONICET, Facultad de Ingeniería, Solís 7575, B7608FDQ Mar del Plata, Argentina

Published online: 30 January 2017

mainly achievable: nanocomposites with either intercalated or exfoliated clay mineral particles. Both structures coexist in nanocomposites, and it suggested that the improvement was ascribed to the dispersion efficiency and the degree of exfoliation of the clay as well as its compatibility with the polymer matrix. In addition to the clays, carbon black also proved to be a suitable filler to produce high thermal stability materials [11]. Consequently, the addition of proper nanoparticles to phenolic resins could increase their thermal stability and mechanical properties to be used in critical applications such matrices of ablative composites [12, 13]. However, since resol-type phenolics have complex 3D structures even prior to cure [14], intercalation of nanoparticles is rather difficult. This limits the number of studies on these resins, compared to other thermosetting resins such as epoxy and unsaturated polyester.

Choi et al. [15] carried out the first study on organoclay reinforced phenolic resin nanocomposites, using novalac-type phenolic resins. They have observed that intercalation of the polymer into the clay galleries occurs during mixing, but there is always the possibility of de-intercalation, and to avoid it, the clay modifier material should always be chosen so that it is either an initiator of the polymerization reaction or some material that reacts with the polymer itself. The structural affinities between the modifier and the polymer, such as benzene rings, have also proven to have a good effect on the intercalation. They also published [16] the mechanical properties and thermal stabilities of the nanocomposites they produced earlier. Byun et al. [17] carried out the first study concentrating on producing nanocomposites from resol-type phenolic resins. They have seen that exfoliation is more difficult with resol than novalac-type phenolic resins, since these resins have a more 3D structure even prior to curing. They have also observed that with increasing amount of clay the enhancement of the properties is lost, mainly due to the defects of stacked silicates and dangling chain formations. Wang et al. [18, 19] synthesized novalac and resol/layered silicate nanocomposites by condensation polymerization of phenol and formaldehyde catalyzed by H-montmorillonite. They found out that the reactants entered the interlayer galleries easily when the condensation polymerization of phenol and formaldehyde is carried out in the presence of montmorillonite. H-montmorillonite, which is actually hydrochloric acid modified montmorillonite, worked as the catalyst for the reaction. Moreover, Bahramian and Kokabi [20] found that the addition of clay Cloisite 15A improves the thermal stability of a resol resin/asbestos composite. This was attributed to the clay platelets which restricted polymer chain motion raising the energy necessary to initiate chain scission and decreased the permeability of the decomposed volatile products. Manfredi et al. [21, 22] and Rivero et al. [23] synthesized resol-based nanocomposites varying the curing and processing conditions, type of clay and organic modifiers. They found that the organically modified montmorillonites showed a better dispersion in the phenolic prepolymer than in the unmodified ones. However, even if the modified montmorillonites showed an interlayer contraction after curing, they were better dispersed when added by mixing with the prepolymer than by in situ polymerization. The nanocomposites with the addition of the unmodified clay showed similar properties independent of the way of synthesis used, which presented the highest cross-linked network. It was stated that independently of the way of synthesis, the type of clay added to the polymer greatly influenced the chemical structure and the final properties of the resol resin.

On the other hand, Natali et al. [24] found that highly loaded carbon black phenolic composites showed superior thermal and dimensional stability than the pristine polymer. More recently, Koo et al. [25] published a review concerning the development of polymer nanocomposites used as thermal protection systems (TPS) analyzing the effect of the addition of different nanoparticles such as organoclays, polyhedral oligomeric silsesquioxanes, carbon black, carbon nano-fibers and nanotubes among others, on the polymeric matrices properties. Furthermore, it was reported [26] that the thermal conductivity and the ablation rate of phenolic composites were reduced with the addition of a variety of nano-materials like nano-silica, montmorillonite.

In spite of the previous works regarding phenolic nanocomposites, no studies concerning the influence of nano-fillers on the kinetics of thermal degradation of the resols were made. So, the aim of the work is to do a comparative study of the effect of different type of nanoparticles on the thermal degradation process of a resol resin, determining the activation energy and the parameters that describe the mentioned process. The accuracy of different kinetics models was analyzed. It is important to know the performance of these nanocomposites because according to the results obtained, some of the systems will be used as matrix in ablative composite materials in a future work.

Experimental

Materials

Phenol crystals and formaldehyde water solution (37 mass%) used for the resol synthesis were supplied by Cicarelli S.A. (Argentina). The reinforcements used were: carbon black (CB) MONARCH 570 supplied by Cabot Argentina SAIC, bentonite (Bent) kindly provided by Minarmco S.A. (Argentina), tributylhexadecylphosphonium bromide modified

bentonite (B-TBHP) according to the conditions detailed in the work [27] and commercial clay Cloisite 30B (C30B) (Southern Clay Products, TX).

Methods

Phenolic resin synthesis

Resol-type phenolic resin was prepared using a formaldehyde to phenol molar ratio equal to 1.3 under basic conditions [28], as follows. Phenol and formaldehyde water solution was placed in a 1 L stainless steel reactor with a low-velocity stirrer, a thermometer and a reflux condenser. The pH was kept at 9.0 with a 40 mass% solution of sodium hydroxide (NaOH), and the mixture was allowed to react for 2 h at 90 °C. After that, the mixture was neutralized with a 7 mass% solution of boric acid until the pH reached a value of 6.8–7.0. The resol was dehydrated in a rotary evaporator by vacuum at 70 °C. The resin obtained was kept at −10 °C until it was used.

Nanocomposites synthesis

Materials were obtained by adding 5 or 20 mass% of different fillers to the original synthesized resol. The addition was performed gradually with continuous stirring and after obtaining homogeneous mixtures, and the mixture was sonicated for 30 min in an ultrasonic bath at room temperature to ensure a good dispersion of the fillers on the resin.

As an alternative to the addition of the nano-clay to the phenolic resin, in order to improve their dispersion, in situ polymerizations were carried out. The procedure was the same as that performed for the synthesis of the neat resol, explained above, with the addition of a sonicated stage at 60 °C during 30 min (the melted phenol with the nano-clay) prior to the addition of the formaldehyde. Then, the mixture obtained was dehydrated in a rotary evaporator by vacuum at 70 °C. Two in situ polymerizations were performed, with modified TBHP bentonite and Cloisite® 30B.

Curing cycle

The nanocomposites obtained by both methods were placed in horizontal molds and cured in electric furnace with an extended cycle in order to obtain materials with low porosity. This cycle is described below and has a similar duration to other chemical systems used in aerospace: 3 h at 40, 60, 80, 100, 130 and 150 °C, and 4 h at 190 °C; the heating rate was 1 °C min^{-1} between each step.

Thermogravimetry

Thermal degradation of the materials was studied by thermogravimetry (TG). Measurements were taken in a Q500 TA Instrument thermogravimetric analyzer. Tests were carried out at heating rates of 5, 10, 15, 20 and 25 °C min^{-1} from 30 to 900 °C, under nitrogen atmosphere. Samples were approximately 10 mg in all cases.

Degradation kinetics: theoretical background

Any solid-state decomposition kinetic can be expresses as a single step kinetic equation:

$$\frac{d\alpha}{dt} = k(T)f(\alpha) \tag{1}$$

where t is time, T is temperature, k is rate constant, $f(\alpha)$ is a differential form of the kinetic model and α is the conversion defined as:

$$\alpha_T = \frac{m_0 - m(T)}{m_0 - m_f} \tag{2}$$

where m_0 and m_f denote the initial and residual mass, respectively, and $m(T)$ refers to the actual mass of the sample. In general, the Arrhenius equation expresses the explicit temperature dependence of the rate constant; therefore, Eq. (1) results in:

$$\frac{d\alpha}{dt} = A\exp\left(\frac{-E}{RT}\right)f(\alpha) \tag{3}$$

where A is a preexponential factor, R is the gas constant and E is the activation energy.

One of the simplest methods to use to determine the activation energies is Kissinger model [29] which is represented by the following Eq. (4):

$$\ln\left(\frac{\beta}{T_{m,i}^2}\right) = \ln\left(\frac{-AR}{E}f'(\alpha_m)\right) - \frac{E}{RT_{m,i}^2} \tag{4}$$

where $f'(\alpha) = df(\alpha)/d\alpha$, β is the heating rate, the subscript m denotes the values related to the rate maximum and the index i is introduced to denote various temperature programs.

Isoconversional methods are frequently called 'model-free methods' because of the absence of any assumptions regarding the mechanisms that take place during the degradation of the samples. These methods give information about of the variation of the apparent activation energy (E_α) as a function of the degree of conversion (α) [30, 31].

In this work, isoconversional methods were employed in order to obtain the E_α. Friedman is the most common differential isoconversional method [32], which can be expressed as:

$$\ln\left(\frac{\mathrm{d}\alpha}{\mathrm{d}t}\right)_{\alpha} = C - \frac{E_\alpha}{RT_\alpha} \tag{5}$$

where $(\mathrm{d}\alpha/\mathrm{d}t)$ is the instantaneous degradation rate as a function of time at a given conversion α, C is a constant and, E_α and T_α are the effective activation energy and the temperature at a certain conversion degree, respectively. At each selected α, the value of E_α can be determined from the slope of a plot of $\ln(\mathrm{d}\alpha/\mathrm{d}t)$ versus $1/T$.

There are a number of integral isoconversional methods which differ in approximations of the temperature integral.

The Kissinger–Akahira–Sunose (KAS) [33] equation can be written as:

$$\ln\left(\frac{\beta}{T^2}\right)_{\alpha} = \ln\left(\frac{AR}{g(\alpha)E_\alpha}\right) - \frac{E_\alpha}{RT_\alpha} \tag{6}$$

where $g(\alpha)$ is the integral conversion function and β is the linear constant heating rate.

Flynn and Wall propose the following approximation:

$$\ln(\beta_\mathrm{i}) = \mathrm{Const} - 1.052\frac{E_\alpha}{RT_\alpha} \tag{7}$$

Vyazovkin developed an advanced integral isoconversional method [34] where the $E\alpha$ value can be determined by minimizing the function expressed by Eq. 8. The temperature integral (Eq. 9) is numerically solved.

$$\zeta(E_\alpha) = \sum_{i=1}^{n}\sum_{i\neq j}^{n}\frac{J[E_\alpha, T_\mathrm{i}(t_\alpha)]}{J[E_\alpha, T_\mathrm{j}(t_\alpha)]} \tag{8}$$

$$J[E_\alpha, T_\mathrm{i}(t_\alpha)] = \int_{t_\alpha-\Delta\alpha}^{t_\alpha} \exp\left(\frac{-E_\alpha}{RT_\mathrm{i}(t)}\right)\mathrm{d}t \tag{9}$$

where i and j denote the different thermal experiments, $\Delta\alpha$ is the conversion increment and $J[E_\alpha,T_\mathrm{i}(t_\alpha)]$ is the temperature integral which can be well approximated with a numeric integral. Subsequently, these data are used to minimize Eq. (8) by seeking an appropriate E_α value. Repeating this minimization procedure for each α of interest, E_α as a function of α will be established.

Estimation of the reaction model and preexponential factor A pair of kinetic parameters (A, E) can be estimated by applying the method of the invariant kinetic parameters (IKP) [35]. Accordingly, sets of $\ln(Ai)$ and Ei are obtained at different heating rates arranging Eq. (3) and replacing $f(\alpha)$ for the most frequently used mechanisms that appear in Table 1:

$$\ln\left(\frac{\mathrm{d}\alpha}{\mathrm{d}T}\frac{\beta_\mathrm{i}}{f(\alpha)}\right) = \ln(Ai) - \frac{Ei}{RT} \tag{10}$$

From the slope and the intercept of plots $\ln[(\mathrm{d}\alpha/\mathrm{d}T)\beta_\mathrm{i}/f(\alpha)]$ versus $1/T$, for each theoretical kinetic model, $f(\alpha)$, and at each heating rate, β, the parameters $\ln(Ai)$ and Ei can be evaluated. Although the parameters vary widely with $f(\alpha)$, generally they all demonstrate a strong correlation known as a compensation effect:

$$\ln(Ai) = a + bEi \tag{11}$$

The parameters a and b are the compensation constants that depend on the heating rate. These lines should intersect in a point that corresponds to the values of E and $\ln A$ for the kinetic model, which were called by Lesnikovich and Levchik the invariant kinetic parameters, E_inv and A_inv that are independent of the conversion, the model and the heating rate [35]. It could be possible that certain variations of the experimental conditions determine regions of intersection. Therefore, the intersection is only approximated. Hence, in order to eliminate the influence of experimental conditions on the determination of A_inv and E_inv, these two parameters are determined from the slope and intersect, respectively, in the so-called supercorrelation relation:

$$a^* = \ln(A_\mathrm{inv}) - b^*E_\mathrm{inv} \tag{12}$$

The IKP method can be used only if E does not depend on α. This fact should be previously checked by isoconversional methods. Once the invariant parameters are obtained, they can be used to estimate the $f(\alpha)$ that best fit the degradation process.

Fourier transform infrared spectroscopy (FTIR)

The degree of cross-linking of the resol in the different materials was analyzed by FTIR. Tests were carried out in a Nicolet 6700 spectrophotometer in the mode of

Table 1 Algebraic expressions for $g(\alpha)$ and $f(\alpha)$ for the most frequently used mechanisms

Mechanism	Symbol	$g(\alpha)$	$f(\alpha)$
1D diffusion	D1	α^2	$1/2\alpha$
2D diffusion	D2	$(1-\alpha)\ln(1-\alpha)+\alpha$	$1/[-\ln(1-\alpha)]$
3D diffusion	D3	$[1-(1-\alpha)^{1/3}]^2$	$(3(1-\alpha)^{2/3})/\{2[1-(1-\alpha)^{1/3}]\}$
4D diffusion	D4	$(1-2\alpha/3)-(1-\alpha)^{2/3}$	$3/\{2[(1-\alpha)^{-1/3}-1]\}$
Avrami–Erofeev, JMA model	A_m $(0.5 \le m \le 4)$	$[-\ln(1-\alpha)]^{1/\mathrm{m}}$	$m(1-\alpha)[-\ln(1-\alpha)]^{(1-1/\mathrm{m})}$
Sestak–Berggren	$\mathrm{SB}_{(\mathrm{n,m})}$		$\alpha^\mathrm{n}(1-\alpha)^\mathrm{m}$

Attenuated Total Reflectance (ATR), with 4 cm^{-1} of resolution and 32 scans.

X-ray diffraction (XRD)

The characterization of the dispersion of the reinforcements in the matrix was carried out by X-ray diffraction. Spectra were obtained with a Panalytical XPERT PRO diffractometer, with CuKα radiation ($\lambda = 1.54$ Å).

Results and discussion

Nano-fillers characterization

Table 2 summarizes the nanoparticles used as fillers of the resol matrix. Regarding clays, it is possible to observe that the unmodified one (Bent) is highly hydrophilic (the absorption of water is higher than 20% after 24 h of exposure), whereas the modified ones (B-TBHP and C30B) became less hydrophilic or more organophilic due to the incorporation of organic cations in the interlaminar space. That modification in the polarity of clays produces changes in their compatibility and the polymeric matrix. The clay C30B was selected because it showed a good dispersion in the phenolic prepolymer [22]. The surfactant based on phosphonium cations to synthesized the B-TBHP was chosen due to its capability as flame retardant [36], taking into account the possible application of the material. Moreover, an increment on the basal or interlaminar spacing which makes room (d_{001}) for the polymeric chains can be achieved by the use of surfactants.

The thermal degradation process of each nano-filler is shown in Fig. 1 (residual mass, TG) and (derivative of mass loss, DTG). It can be observed that the thermal stability of unmodified clay is clearly higher than that of the modified ones, which is related to the degradation of organic modifiers at lower temperatures (between 200 and 500 °C). In the case of clays, one interesting result from TG experiments is that the water content (obtained from residual mass curve until 130 °C) undoubtedly decreased in both modifications. This, in turn, indicates an enhancement on the hydrophobicity which is in accordance with water absorption results (Table 2). In addition, it can be observed that the thermal stability of phosphonium modified clays is higher than that of the ammonium modified ones and both are lower than the unmodified bentonite. Several authors [37, 38] have suggested different steps on the degradation mechanism of bentonites and montmorillonites modified with quaternary ammonium salts. In the case of carbon black, there are no evident peaks which, in turn, are associated with the high thermal stability of that filler.

All previous description will affect the results of the thermal degradation process of resol/nano-filler composites that will be described in the following section.

Effect of nanoparticles on the thermal degradation of the resol resin

To study the overall degradation process of the materials, thermogravimetric curves obtained at 10 °C min^{-1} were analyzed. For that, curves of residual mass as a function of temperature, and its derivative (DTG) as a function of temperature were plotted for each nanocomposite and compared with that of the neat resol. In order to determine the influence of the filler content on the thermal behavior of the neat resol, two different nanoparticles contents (5 and 20 mass%) were studied.

Thermal degradation of phenolic resin shows three main regions: (a) from 250 to 400 °C where the postcuring and oxidative degradation with the evolution of formaldehyde, water and carbon dioxide, (b) from 400 to 600 °C where the thermal fragmentation releasing phenol, cresol, xylenol and (c) from 500 to 750 °C where the carbon char is formed producing H_2, CO and CH_4 (Fig. 2). The involved reactions are numerous, and they are well known [39].

Table 2 Characteristics of the fillers used in the nanocomposites

Filler	Organic modifier	Abs. water 24 h at 90% *RH*[b]/%	d_{001}/nm	Mass loss on ignition/%	T_p TG/°C
Bent	None	21.22	1.17	11	625
B-TBHP	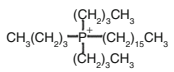	2.73	2.51	25	396
C30B	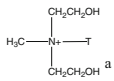 [a]	3.72	1.85	30	275
CB	None	–	300 (size)	2.4	–

[a] *T* tallow (65% C18; 30% C16; 5% C14)

[b] *RH* relative humidity

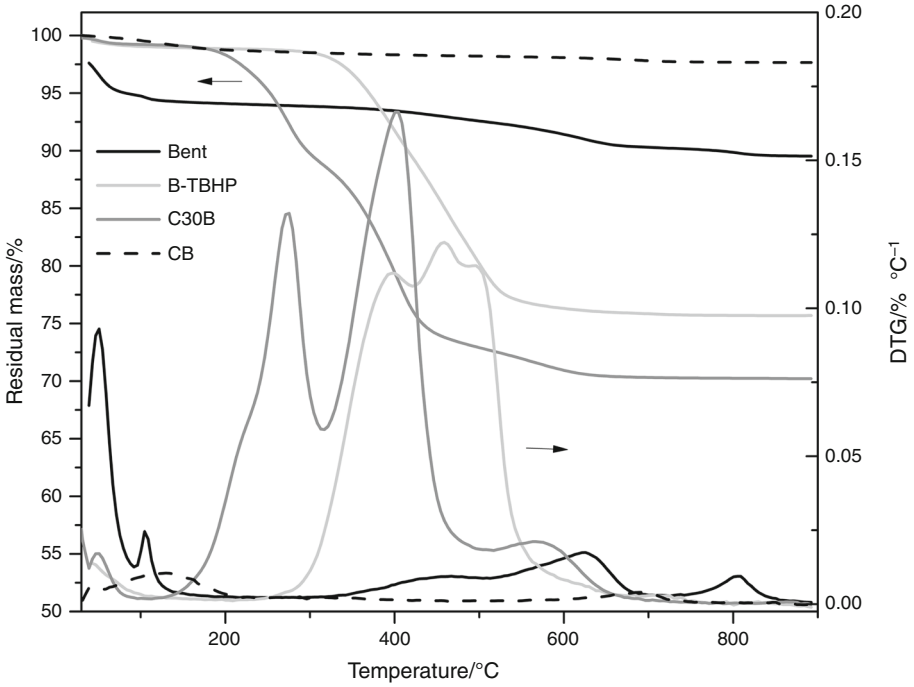

Fig. 1 Residual mass as a function of temperature (TG) of different nanoparticles used as filler of resol matrix and derivative of the residual mass as a function of temperature (DTG) of different nanoparticles used as filler of resol matrix

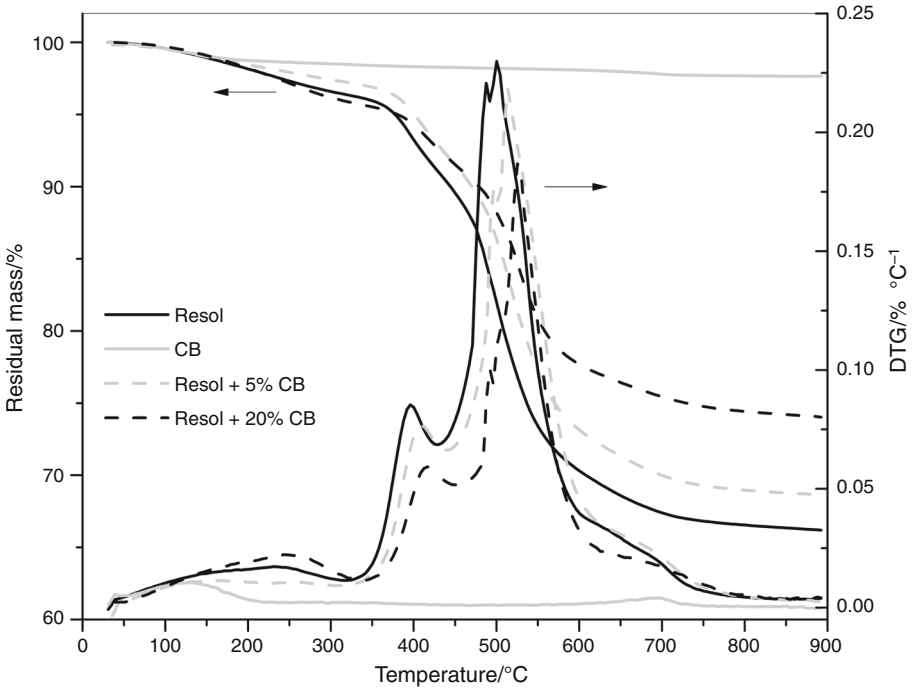

Fig. 2 TG and DTG curves for resol and carbon black/resol resin nanocomposite in nitrogen atmosphere

Regarding the nanocomposites, it can be observed from Fig. 2 that the addition of carbon black to the resol matrix generates an improvement on its thermal stability, evidenced by the displacement of the mass loss stages to higher temperatures and also by an increase in the residual mass (10% average) at the end of the test. This behavior was more evident with the increase in the carbon black content (5–20 mass%), and it could be associated with the fact that the carbon black promotes the char formation, creating a protective layer which acts as a barrier between the material and the heat source. It was reported that the presence of carbon black substantially lower yields of volatile products [40]. Thermogravimetric curves exhibit the same profile, and the decomposition takes place via similar stages, suggesting that the resol and its nanocomposites with CB follow a similar degradation mechanism.

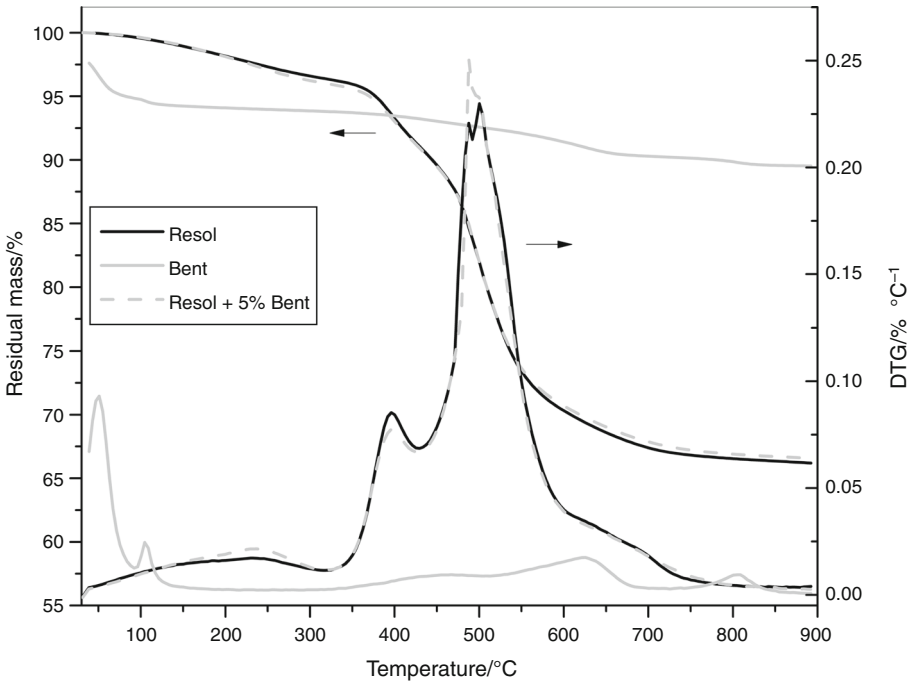

Fig. 3 TG and DTG for resol and bentonite/resol resin nanocomposites in nitrogen atmosphere

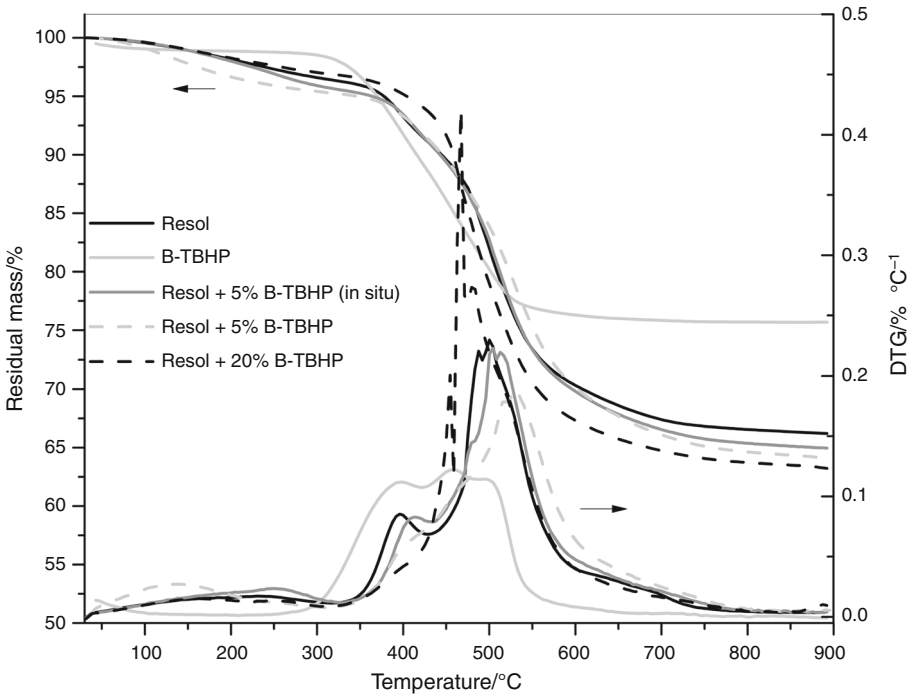

Fig. 4 TG and DTG for resol and B-THBP/resol resin nanocomposites in nitrogen atmosphere

The results of the thermogravimetric analyses of the composites containing bentonite, bentonite modified with TBHP and C30B are shown in Figs. 3–5, respectively. It can be observed that the addition of all used clays did not appreciably modify the thermal degradation process of the resin. However, the addition of bentonite with TBHP (Fig. 4) slightly delays the beginning of the thermal degradation process, but reduces the thermal stability of the resol at temperatures higher than 450 °C when the clay content was raised to 20 mass%. In general, nanocomposites with clay showed lower residual mass than the resol probably due to a lower cross-linking caused by the filler addition [22, 41], which was analyzed by FTIR and discussed later. Table 3 shows a summary of the results from the thermogravimetric analyses of the materials studied, where the increase in the residual mass due to the carbon black addition is evidenced.

Table 3 Characteristic temperatures obtained by thermogravimetry for the materials studied

Material	$T_{5\%}$/°C	$T_{10\%}$/°C	T_{dmax}/°C	Residue at 800 °C/%
Resol	466	496	500	66.5
Resol + 5% CB	467	505	513	69
Resol + 20% CB	492	525	525	74
Resol + 5% Bent	467	496	488	67
Resol + 5% C30B	450	485	485	64
Resol + 20% C30B	434	459	467	60
Resol + 5% C30B (in situ)	459	492	504	65
Resol + 5% B-TBHP	465	505	530	65
Resol + 20% B-TBHP	459	475	479	64
Resol + 5% B-TBHP (in situ)	463	500	504	65

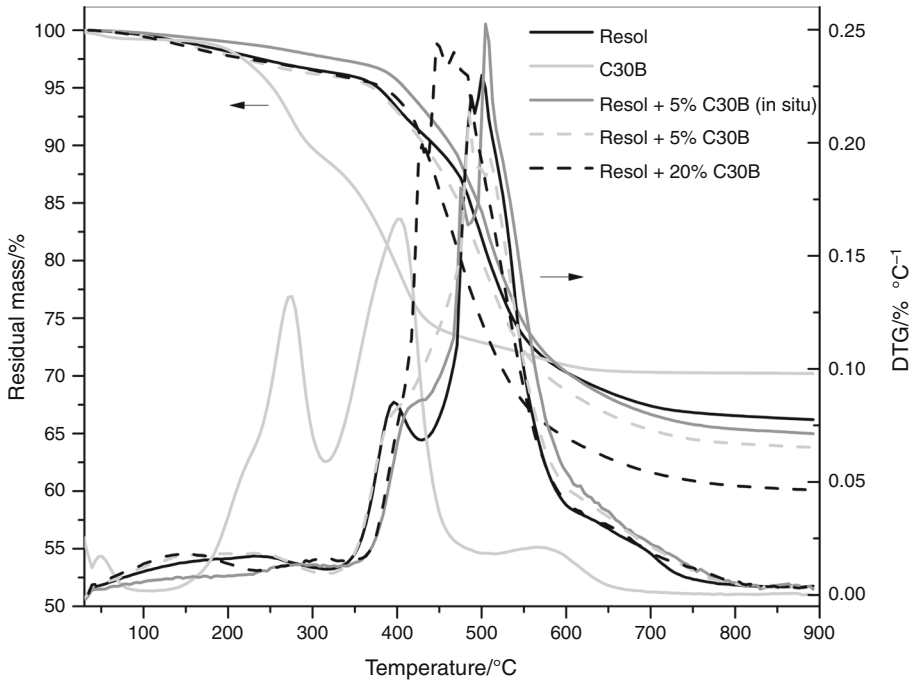

Fig. 5 TG and DTG for resol and C30B/resol resin nanocomposites in nitrogen atmosphere

However, no significant enhancement in the thermal stability of the nanocomposites was observed by increasing the filler content. Furthermore, the nanocomposites with 20% of the modified clays showed a slight detriment in the overall thermal performance compared with the ones with lower nanoparticle content. This could be related to differences in the cross-linking density of the resol and with the dispersion of the particles in the polymer.

Considering the addition of higher percentages of nanoparticles did not significantly improved the thermal stability of the nanocomposites. The following work concerning the kind of processing, chemical characterization and thermal degradation kinetics of the polymer was done considering only the nanocomposites with the lower content of nanoparticles.

Effect of processing on the thermal degradation of resol nanocomposites

In order to analyze the influence of the processing method on the thermal behavior of the clay-based nanocomposites, in situ polymerization was performed for the preparation of composites containing C30B and bentonite modified with TBHP.

XRD profiles of the nanocomposites, showed in Fig. 6, revealed that the in situ addition of the clay did not improve their dispersion in the polymer compared with the mixed ones. No peaks at low angles were distinguished for the latest which in turn indicates an increase on the interlaminar spacing of the clay that can be associated with the intercalation of polymeric chains into the clay galleries

[42]. However, the composites obtained by in situ polymerization showed broader peaks which represent an inhomogeneous interlaminar spacing of the clay platelets, i.e., the coexistence of regions where the clay is better distributed together with more agglomerated zones. Moreover, a displacement of the peak to higher angles was also observed for these composites which are an indication of a contraction of part of the clay galleries. This could be attributed to the loss of surfactant during curing or to a different rate of resol curing inside and outside the galleries [23]. In spite of the differences in the clay dispersion, the thermal degradation analysis of the composites obtained by in situ polymerizations (Figs. 4, 5) reveals similar results to those discussed above, no significant improvements were found in the mass loss areas and the residual mass of the samples at the end of the test. These results are also included in Table 3.

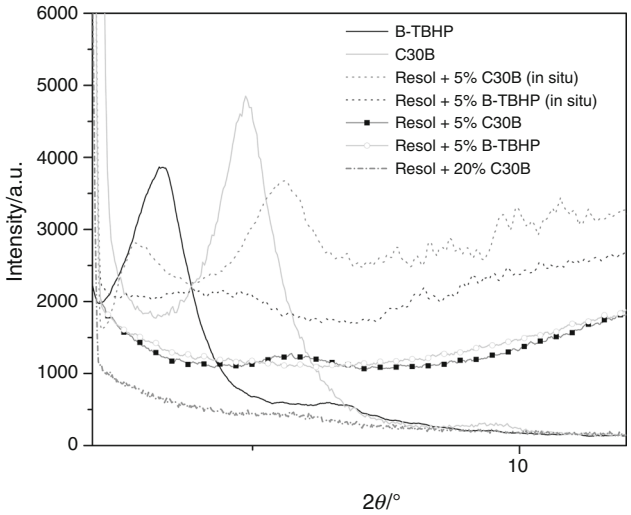

Fig. 6 XRD profiles of the C30B, B-TBHP and the 5 mass% clay-based nanocomposites obtained by mixing and in situ polymerization

Figure 7 shows the DTG curves of the resol-based nanocomposites together containing 5 mass% of the different nanoparticles in order to compare their thermal degradation performance. It was observed that the carbon black was the most efficient nano-reinforcement increasing the onset temperature and the quantity of char residue. In addition, the bentonite modified with TBHP showed a better behavior than the C30B on the resol thermal degradation. This was attributed to the high thermal stability of the phosphonium modifier compared to the ammonium-based one, as it was observed in Fig. 1.

FTIR tests were carried out to analyze the influence of the nanoparticles on the cross-linking density of the original phenolic resin. For this, the chemical structure of the polymer was analyzed taking into account the typical groups of the phenolic resin as the methylene bridges, which are formed during the cross-linking reactions. Methylene bridge bands are situated at wavelengths of 1450 and 1473 cm^{-1}, for *para–para′* and *ortho-para′* bridges, respectively [28]. The obtained spectra were normalized with the peak situated at 1600 cm^{-1} that corresponds to the stretching of the aromatic ethylene bond C=C in the aromatic ring which seems to be constant during all the tests [28]. The cross-linking density of the resol in the different materials was estimated as the height of the peak at 1473 cm^{-1} and compared among them. The results are shown in Table 4. It can be observed that in all the cases, the fillers reduced the cross-linking density of the resin, and this was associated to the fact that the particles acts as a physical impediment during polymerization, modifying the polymerization rate as it was explained previously.

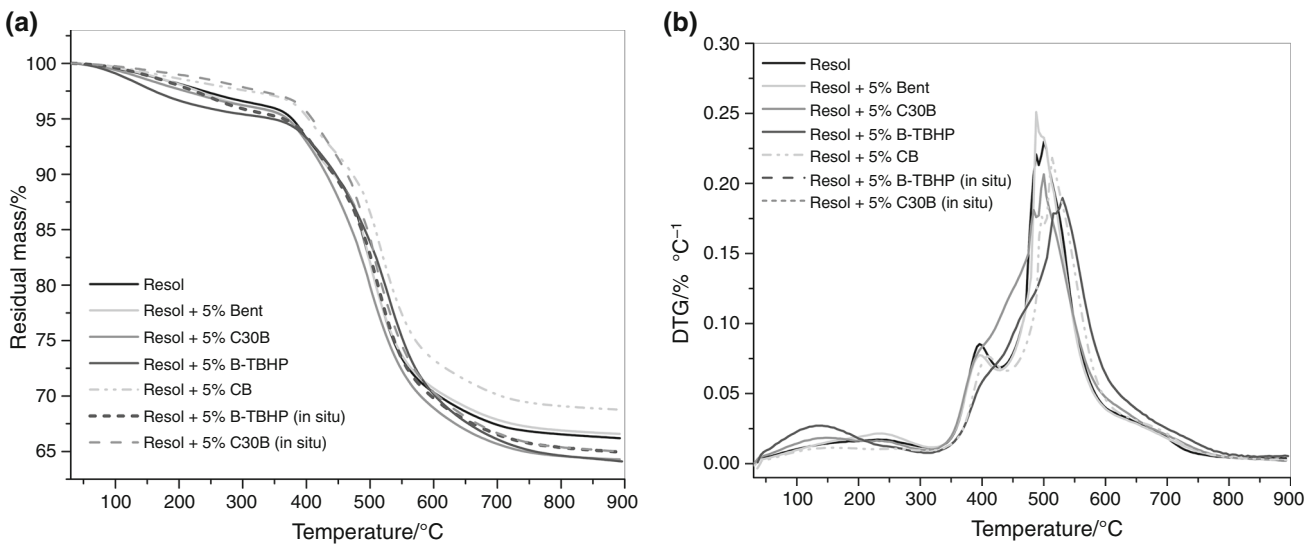

Fig. 7 **a** TG and **b** DTG for resol and phenolic resin nanocomposite with 5 mass% of the different nanoparticles in nitrogen atmosphere

Additionally, the lower cross-linking density obtained with the modified clays could be attributed to the presence of the long carbon chains of the surfactants producing more free volume [23].

Kinetic analysis and modeling of the thermal degradation process

The kinetic degradation analysis was performed taking into account the two peaks that appears in the DTG curves in the range between 350 and 600 °C, where the most significant structural changes take place, as it was previously explained. So, these peaks were deconvoluted by a Lorentzian multi-peak curve, and the whole degradation process was divided in two parts (P1 and P2), each one associated to one of the degradation peak where the conversion degree values vary between 0 and 1. Only the second peak was considered for the nanocomposite with B-TBHP because the first one only appears as a shoulder in the DTG curves and did not fit the model (Fig. 7b). Figure 8 displayed the application of the Kissinger model to the resol resin, as an example. An acceptable linearity of the curves was observed for the first and second peak, and the apparent activation energies are reported in Table 5.

The results obtained from the application of Flynn and Wall method to the dynamic DTG data for both peaks of the resol are reported in Fig. 9a (P1) and b (P2), as an example. It was observed that no good linearly fit was reached from the experimental values calculated for the samples at the different conversions. Moreover, an increment in the activation energy with the conversion was found, because of the occurrence of more cross-linking reactions that take place during the degradation process.

Table 4 Relative peak heights obtained by FTIR

Material	$H_{1473\ cm^{-1}}/H_{1600\ cm^{-1}}$
Resol	2.60
Resol + 5% C30B	1.83
Resol + 5% CB	1.64
Resol + 5% B-TBHP	0.79
Resol + 5% Bent	0.78

Table 5 Apparent activation energies calculated from Kissinger method

Material	Apparent activation energy, *Ea*/kJ mol^{-1}	
	First peak	Second peak
Resol	266.1	283.9
Resol + 5% Bent	264.3	339.2
Resol + 5% B-TBHP	–	311.4
Resol + 5% C30B	268.9	289.0
Resol + 5% CB	270.2	288.0

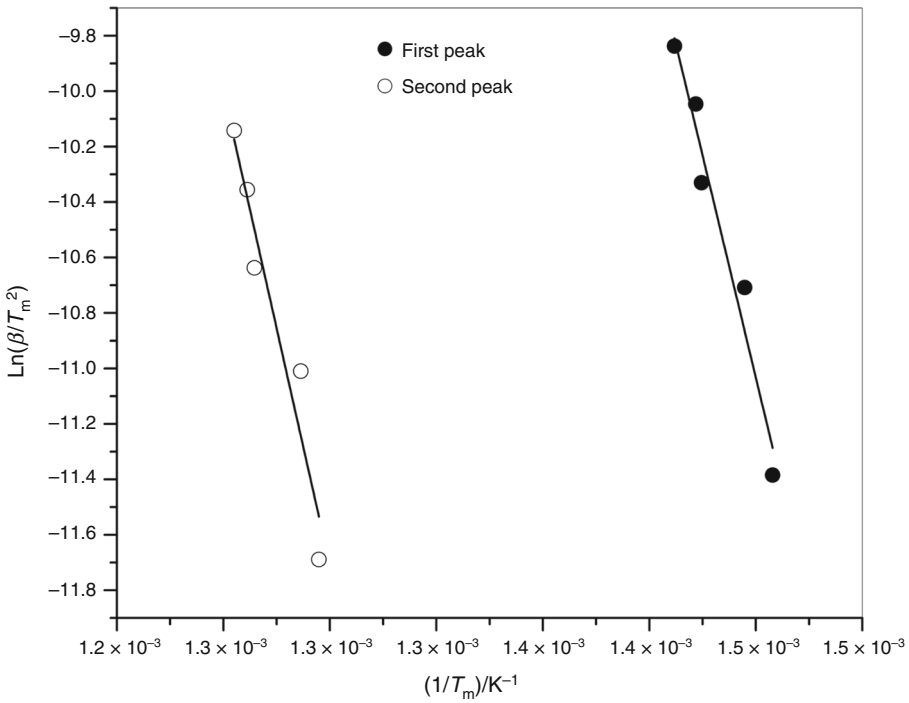

Fig. 8 Results of Kissinger method to resol resin, both peaks

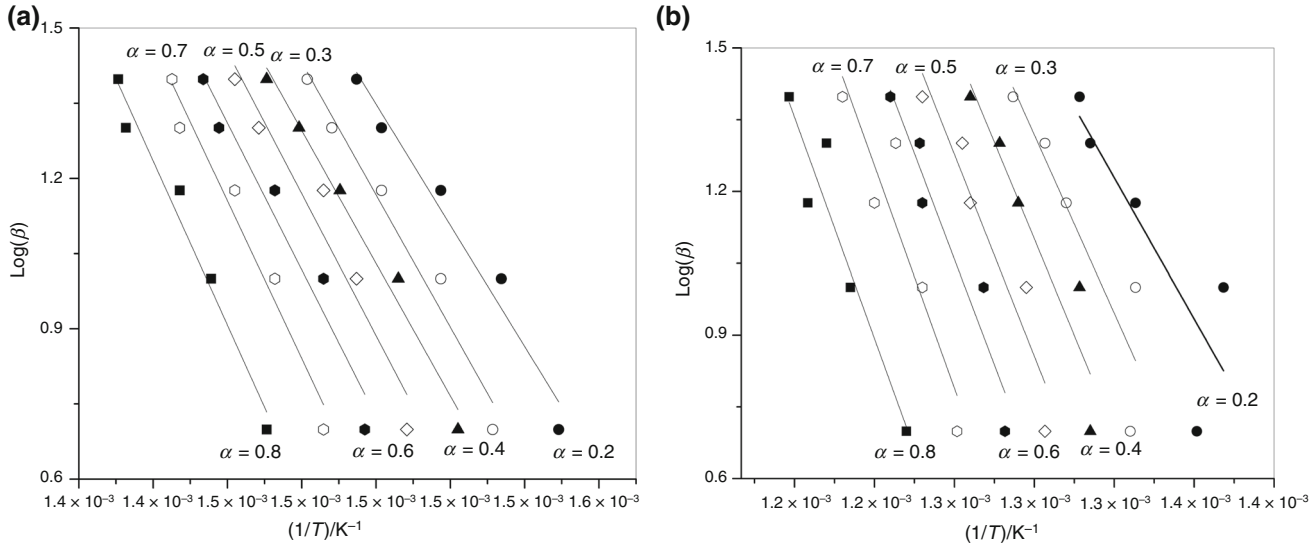

Fig. 9 Application of Flynn and Wall method to resol: **a** P1; **b** P2

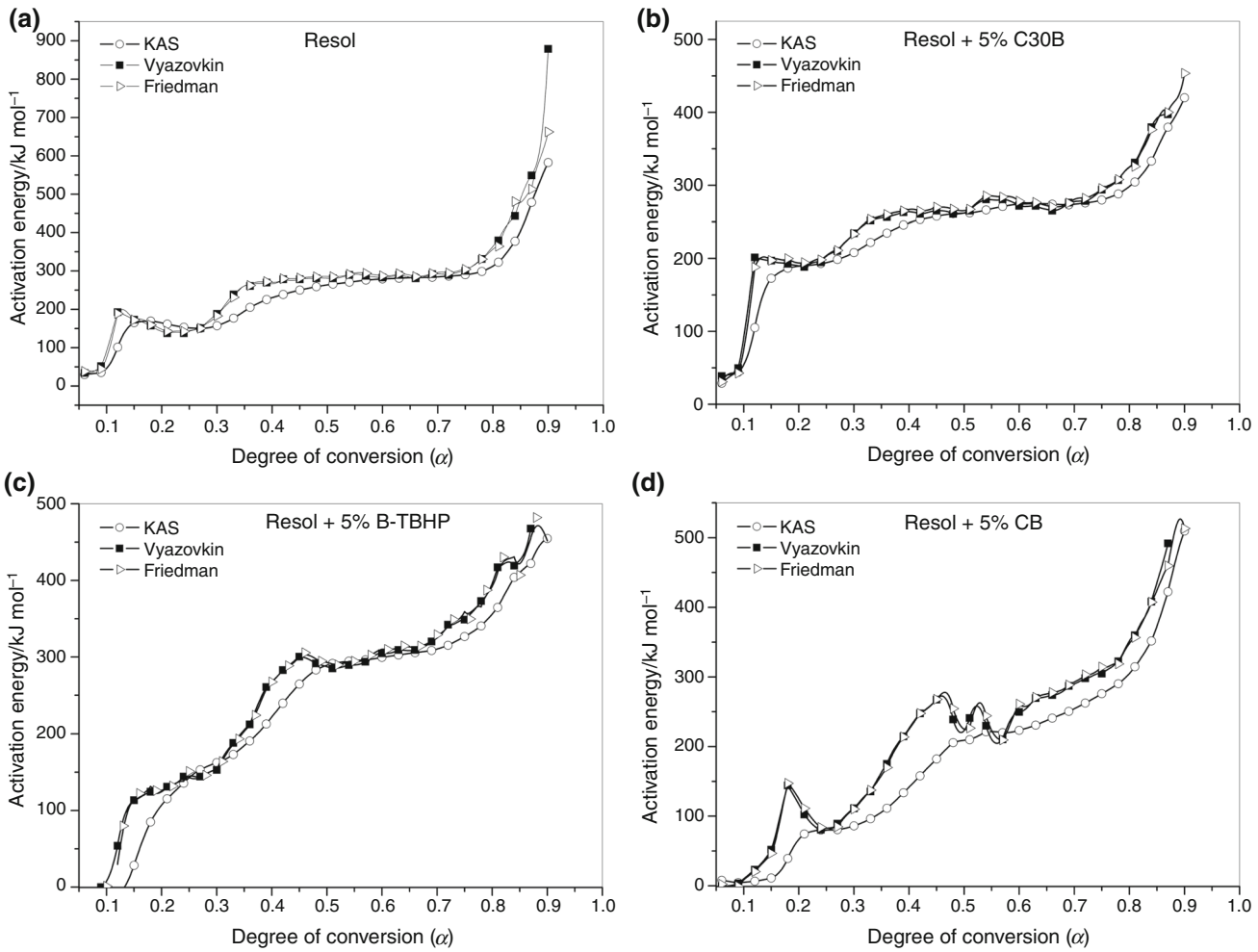

Fig. 10 Apparent activation energy versus degree of conversion applying KAS, Vyazovkin and Friedman methods for: **a** resol, **b** resol + 5% C30B, **c** resol + 5% B-TBHP, **d** resol + 5%CB

So, it can be concluded that those models are not suitable to calculate the kinetic parameters of the studied system. The calculated activation energies have too much error and do not allow a comparative analysis among the materials.

In order to determine realistic and accurate kinetic triplet for non-isothermal degradation of the materials, isoconversional methods were used. These methods allow verification of the presence or absence of the complexity of investigated process, tested from the mechanistic point of view. The whole thermal degradation process (without deconvolution procedure) was evaluated by means of three widely used isoconversional methods. The variation of the apparent activation energy with the conversion for the materials studied was calculated by Friedman, KAS and Vyazovkin methods. Figure 10 shows the results obtained, and it was observed that the E_α values calculated by Vyazovkin and Friedman are practically identical because the integration was done using small intervals of conversion ($\Delta\alpha = 0.01$) [26]. However, differences among the E_α calculated by Friedman method and those integral such as Vyazovkin and KAS were reported when higher intervals of α were employed [43, 44]. On the other hand, it was reported [26] that the Vyazovkin method, which uses numerical integration, shows further increase in accuracy than the KAS one. Therefore, the apparent activation energy for the thermal degradation calculated by the Vyazovkin method in resol and its nanocomposites was considered for the discussion.

It was observed in Fig. 11 that the E_α values for the resol varied between 35 and 290 kJ mol^{-1} up to 0.75 degree of conversion and then raised sharply. This behavior could be related to the degradation steps of the phenolic resin observed by TG, which were explained above. E_α value showed a first increase up to $\alpha = 0.14$ which could be associated to postcuring reactions, and then, it drops up to $\alpha = 0.25$ due to the gas evolution (formaldehyde, water and carbon dioxide). When $\alpha > 0.25$ the E_α value showed first a steep increase and then continues with slowly increase till $\alpha = 0.75$. It was associated to the thermal fragmentation zone, which involved fragmentation reactions and the development of further cross-linking. That shape of the curve is characteristic of a complex mechanism involving competing reactions [45, 46]. After $\alpha = 0.75$, the E_α increased because the system needs more energy for degradation due to the surface protecting layer of char formed which restricts further degradation.

The variation of the activation energy with the conversion for the resol and the different nanocomposites containing 5% of nanoparticles was showed in Fig. 12. It was observed a similar shape among the curves of the nanocomposites and the resol, indicating a similar degradation mechanism. All the materials exhibited a rise in the activation energy at the beginning of the degradation process due to the DTG peak corresponding to the release of water and oligomers, as shown in Fig. 7b. At α higher than 0.75, the nanocomposites showed less E_α than the resol because of their minor cross-linking density estimated by FTIR. Additionally, the variation of the activation energy for the composite with CB was displaced to the right, consistent with its higher thermal stability.

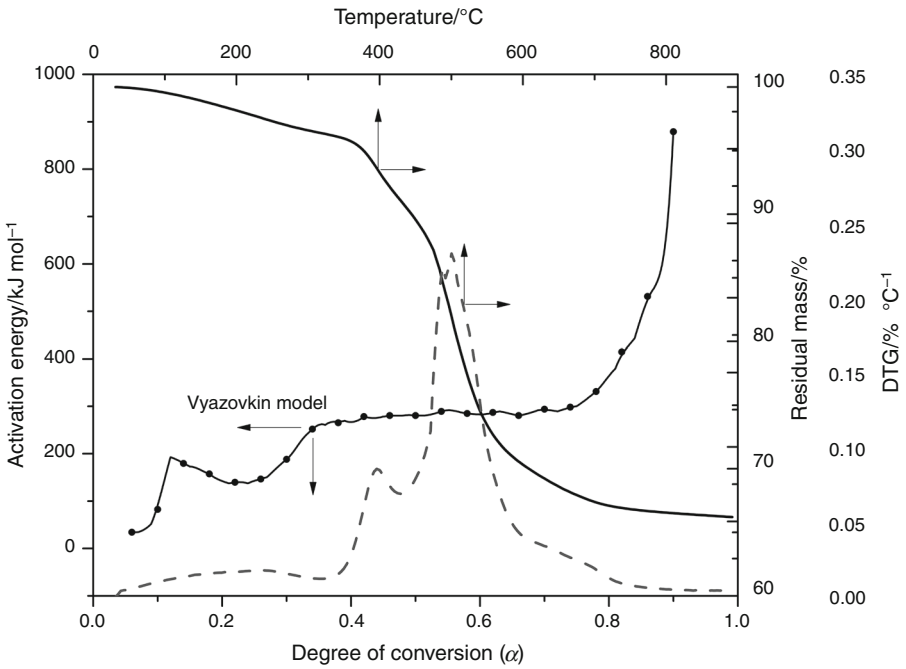

Fig. 11 Comparison of apparent activation energy versus degree of conversion applying Vyazovkin method, and curves of resol

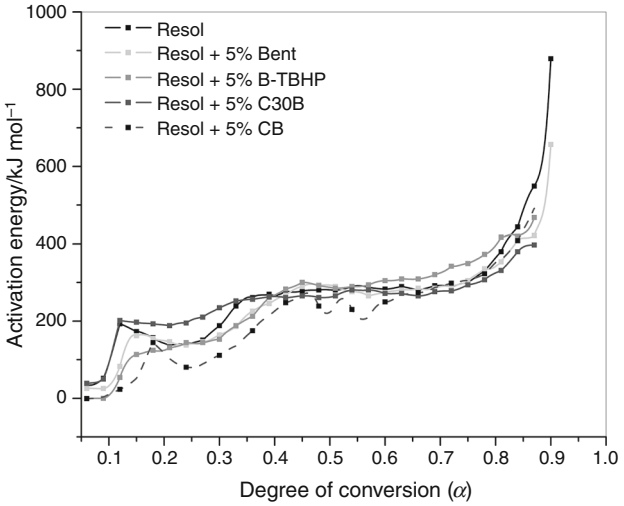

Fig. 12 Apparent activation energy versus degree of conversion for the resol and the nanocomposites with 5% of nanoparticles, applying the Vyazovkin method

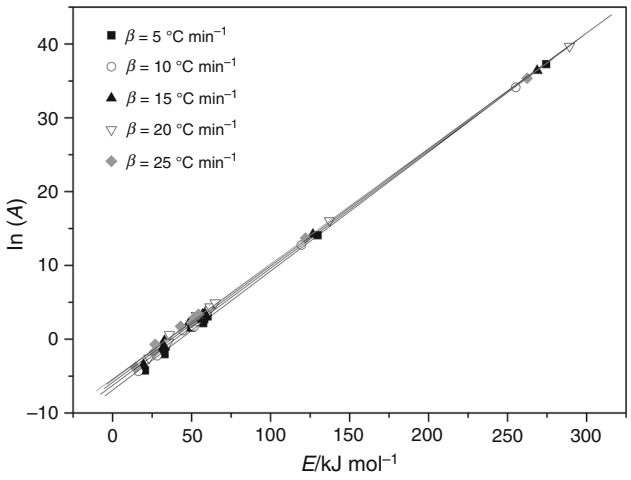

Fig. 13 Compensation effect for degradation of resol + 5% C30B (P1) using models type A_m, $SB_{(n,m)}$

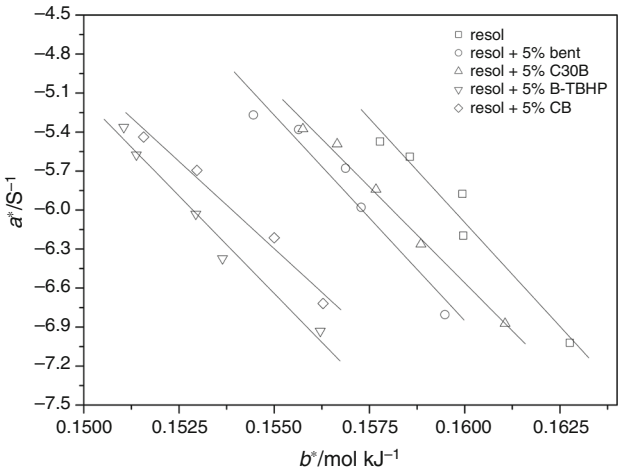

Fig. 14 Supercorrelation relationship for resol and its nanocomposites for peak 2

Estimation of the invariant kinetic parameters (IKP)

In order to determine the invariant kinetic parameters and evaluate which kinetic model best describes the thermal degradation process of the studied systems, the IKP method was used. This method was applied to the two deconvoluted peaks (P1 and P2) representing the whole degradation process, as explained above. The IKP method could be applied because it was observed by an isoconversional method (Fig. 12) that the activation energy does not depend on α in the conversion range comprising P1 and P2. Algebraic expressions for the kinetic models usually used in the solid-state kinetics are shown in Table 1. Substitution of different models $f(\alpha)$ (type A_m, with $m = 0.5$, 1, 2, 3, 4; $SB_{(n,m)}$ with n, $m = 0.4$, 0.3; 0.6, 0.4; 0.4, 0.4; 0.5, 0.5) in Eq. (3) and fitting it to experimental data yields different pairs of the Arrhenius parameters, ln(A) and E. Diffusion models were not employed in order to improve the quality of the correlation [47]. The compensation effect between E and ln (A) was checked in the different models at all heating rates, in all the studied systems. Figure 13 shows, as an example, the compensation relationship for the non-isothermal degradation of resol + 5% C30B (P1). The same compensation effect was obtained from all the resol nanocomposites. The slopes and intercepts of these lines give the compensation parameters a and b at each heating rate. Since determining the intersection of these lines by the graphical method is uncertain, the calculation of the invariant kinetic parameters is performed using the supercorrelation relation, Eq. (12). Figure 14 exhibits the results of a^* and b^* for peak 2 for the resol and its nanocomposites, showing very good straight lines for all specimens investigated, thus proving the existence of a supercorrelation relation. The evaluation of E_{inv} and A_{inv} was done from the slope and the intercept of the lines in Fig. 14, respectively. Additionally, it was corroborated that the isokinetic temperature ($T_{iso} = 1/R\ b$) is within the experimental range of degradation temperatures as a criterion to validate model application [48]. The calculated T_{iso} values vary from 467 to 523 °C.

In the same way, the existence of the compensation effect between E and ln(A) and the one-step process were confirmed for P1 in all nanocomposites. The values of the invariant parameters estimated for both peaks are shown in Table 6. All activation energy values were similar in the vicinity of 290 kJ mol^{-1}, which are in very good agreement with estimated values presented in the previous section.

In order to estimate the reaction model, $f(\alpha)$, which best describes the experimental data, the Avrami–Erofeev and

Table 6 Values for the invariant kinetic parameters for resol and its nanocomposites

Material	First peak rel. area	Second peak rel. area	Ln (A_{inv})/s^{-1}		E_{inv}/kJ mol^{-1}		R^2	
	P1	P2	P1	P2	P1	P2	P1	P2
Resol	0.184	0.816	37.88	45.05	280.07	319.67	0.976	0.98
Resol + 5% Bent	0.176	0.824	44.18	43.74	318.97	316.21	0.974	0.97
Resol + 5% C30B	0.138	0.862	38.88	40.62	283.83	294.87	0.994	0.995
Resol + 5% THBP	0.116	0.884	39.88	39.89	300.18	300.21	0.989	0.989
Resol + 5% CB	0.195	0.805	35.84	35.33	271.84	268.57	0.987	0.989

Table 7 Values for n and m exponents from the Sestak–Berggren kinetic model for resol and its nanocomposites

Material	$n_{average}$		$m_{average}$	
	P1	P2	P1	P2
Resol	−0.5	−0.491	2.42	4.667
Resol + 5% Bent	−0.738	−0.727	3.107	3.042
Resol + 5% C30B	−0.763	−0.819	3.048	3.23
Resol + 5% TBHP	−0.993	−0.992	4.47	4.484
Resol + 5% CB	−0.558	−0.543	2.593	2.518

Sestak–Berggren models (Table 1) were evaluated. So as to choose among these two models, the criterion suggested by Perez-Maqueda et al. [49] was used. They stated that when the correct kinetic model is assumed for $f(\alpha)$, all experimental data points should lie on a single straight line by plotting $\ln[(d\alpha/dt)\beta/f(\alpha)]$ versus $1/T$. The slope and the intercept of this line should provide the same values of the activation energy and preexponential factor as the initially assumed. It was observed that the Avrami–Erofeev model did not result in a single straight line after applying this procedure using several m values, for both peaks (P1 and P2) in all the materials studied. Instead, it was possible to obtain a straight line by applying the Sestak–Berggren model, considering several n and m values.

Then, to estimate the best n and m exponents of the Sestak–Berggren kinetic model, a nonlinear regression analysis was applied for $f_{inv}(\alpha)$ function (Eq. 13), using the experimental data and the invariant parameters:

$$f_{inv}(\alpha) = A_{inv}^{-1} \exp\left(\frac{E_{inv}}{RT}\right) \beta \frac{d\alpha}{dT} \tag{13}$$

The average values of n and m are listed in Table 7. The correlation coefficient, R^2, in the fitting procedure was excellent (0.99>) in all the cases.

To verify that all experimental data points lie on a single straight line with the average n and m values calculated, plots of $\ln[(d\alpha/dt)\beta/f(\alpha)]$ versus $1/T$ were constructed. Such plots for resol + 5% C30B and resol + 5% TBHP at different heating rates for peak 1 appear in Fig. 15a.

Additionally, the experimentally obtained differential ($d\alpha/dT$ vs. T) was compared with the modeled one in order to confirm the selected kinetic model (Fig. 15b). The $d\alpha/dT$ was simulated using the kinetic triplets, which were calculated as follows: the preexponential factor was

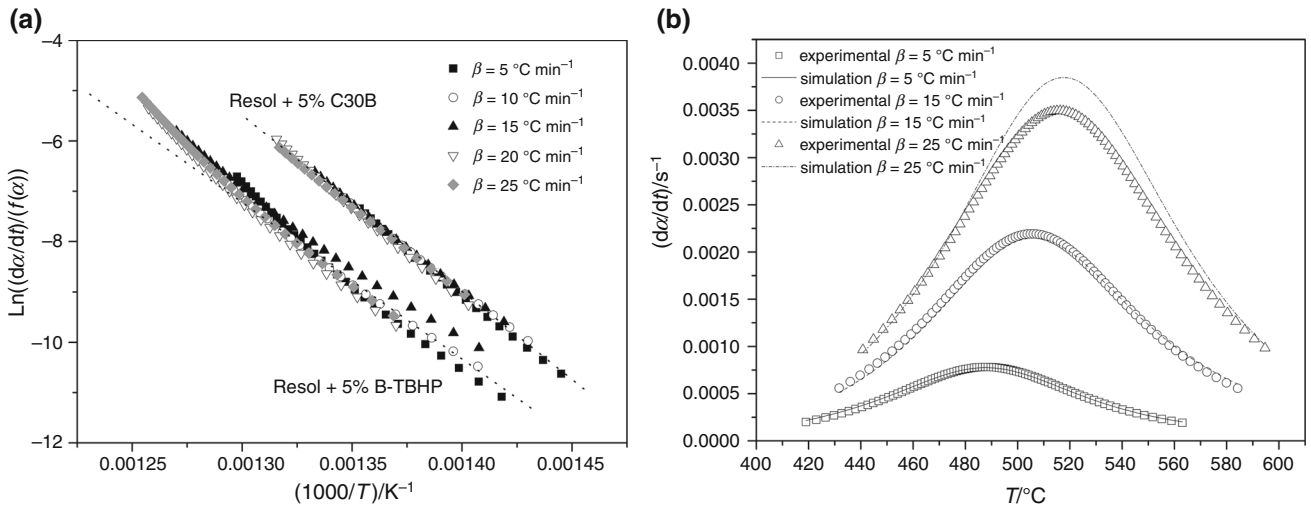

Fig. 15 **a** Plots of $\ln[(d\alpha/dt)\beta/f(\alpha)]$ versus $1/T$ for resol + 5% C30B and resol + 5% B-TBHP, for P1, **b** comparison between the experimentally obtained differential degradation curves and the calculated degradation curves of resol + 5% C30B (P2)

obtained using the C values from the Friedman method (Eq. 5) and the selected $f(\alpha)$. The apparent activation energy profile, also derived from Friedman method, was used. Figure 15b clearly shows that the experimental differential degradation curves are successfully simulated by means of the above calculated kinetic parameters.

Conclusions

In this work, the effect of different contents and types of nano-fillers on the thermal degradation of phenolic resin were studied by TG. It was found that the carbon black was the most effective filler in improving the thermal stability of the phenolic matrix, evidenced by the displacement of the mass loss stages to higher temperatures and also by an increase in the residual mass at the end of the test. This result was associated with the fact that the carbon black promotes the char formation and besides, it is more compatible with the polymer.

The kinetic degradation analysis of the resol and the nanocomposites was performed by means of three widely used isoconversional methods: Friedman, KAS and Vyazovkin. The profile of the apparent activation energy with the conversion calculated by Vyazovkin model, the most accurate method, was correlated with the degradation steps of the phenolic resin observed by TG. The shape of the curve in the thermal fragmentation zone, between 350 and 600 °C, was characteristic of a complex mechanism involving competing reactions. Above that temperature, the E_α increased because the system needs more energy for degradation due to the char layer formed in the surface. The curves of the nanocomposites exhibited a similar shape to resol, thus indicating a comparable degradation mechanism. Moreover, the activation energy profile of the composite with CB was displaced to the right, consistent with its higher thermal stability.

In order to estimate a pair of kinetic parameters (A, E_α), the method of the invariant kinetic parameters (IKP) was applied considering the two deconvoluted peaks in the thermal fragmentation zone, representing the whole degradation process. The invariant activation energies calculated in all the samples were in accordance with the ones estimated by the isoconversional methods. Then, it was determined that the Sestak–Berggren model best describes the thermal degradation experimental data, and the average reaction order values (n and m) were reported in all the systems. Finally, a comparison between the experimentally obtained and the simulated differential degradation curves indicates that the resulted model was certainly accurate to predict the thermal degradation process of the resol and the nanocomposites.

Acknowledgements The authors would like to thank the Consejo Nacional de Investigaciones Científicas y Técnicas (CONICET), Agencia Nacional de Promoción Científica y Tecnológica (ANPCyT) (PICT'12-1983; PICT2013-2455) and Universidad Nacional de Mar del Plata (15/G378).

References

1. Gardziella A, Pilato LA, Knop A. Phenolic resins. 2nd ed. Berlin: Springer; 2000.
2. Lan T, Pinnavaia TJ. Clay-reinforced epoxy nanocomposites. Chem Mater. 1994;6:2216–9.
3. Vaia RA, Price G, Ruth PN, Nguyen HT, Lichtenhan J. Polymer/layered silicate nanocomposites as high performance ablative materials. Appl Clay Sci. 1999;15:67–92.
4. Zilg C, Thomann R, Finter J, Mülhaupt R. The influence of silicate modification and compatibilizers on mechanical properties and morphology of anhydridecured epoxy nanocomposites. Macromol Mater Eng. 2000;280:41–6.
5. Sun Y, Zhang Z, Moon KS, Wong CP. Glass transition and relaxation behavior of epoxy nanocomposites. J Polym Sci Part B Polym Phys. 2004;42:3849–58.
6. Yasmin A, Luo JJ, Abot JL, Daniel IM. Mechanical and thermal behavior of clay/epoxy nanocomposites. Compos Sci Technol. 2006;66:2415–22.
7. Hsiue GH, Liu YL, Liao HH. Flame-retardant epoxy resins: an approach from organic–inorganic hybrid nanocomposites. J Polym Sci Part A Polym Chem. 2001;39:986–96.
8. Balabanovich AI, Hornung A, Merz D, Seifert H. The effect of a curing agent on the thermal degradation of fire retardant brominated epoxy resins. Polym Degrad Stab. 2004;5:713–23.
9. Ha SR, Ryu SH, Park SJ, Rheed KY. Effect of clay surface modification and concentration on the tensile performance of clay/epoxy nanocomposites. Mater Sci Eng A. 2007;448:264–8.
10. Guo B, Jia D, Cai C. Effects of organo-montmorillonite dispersion on thermal stability of epoxy resin nanocomposites. Eur Polym J. 2004;40:1743–8.
11. Visakh PM, Arao Y. Thermal degradation of polymer blends, composites and nanocomposites. Cham: Springer; 2015.
12. Naderi A, Mazinani S, Javad Ahmadi S, Sohrabian M, Arasteh R. Modified thermo-physical properties of phenolic resin/carbon fiber composite with nano zirconium dioxide. J Therm Anal Calorim. 2014;117(1):393–401.
13. Amirsardari Z, Aghdam RM, Salavati-Niasari M, Shakhesi S. Preparation and characterization of nanoscale ZrB2/carbon–resol composite for protection against high-temperature corrosion. J Therm Anal Calorim. 2015;120(3):1535–41.
14. Wolfrum J, Ehrenstein GW. Interdependence between the curing, structure and the mechanical properties of phenolic resins. J Appl Polym Sci. 1999;74:3173–85.
15. Choi MH, Chung IJ, Lee JD. Morphology and curing behaviors of phenolic resin-layered silicate nanocomposites prepared by melt intercalation. Chem Mater. 2000;12:2977–83.
16. Choi MH, Chung IJ. Mechanical and thermal properties of phenolic resin-layered silicate nanocomposites synthesized by the melt intercalation. J Appl Polym Sci. 2003;90:2316–21.
17. Byun HY, Choi MH, Chung IJ. Synthesis and characterization of resol type phenolic resin/layered silicate nanocomposites. Chem Mater. 2001;13:4221–6.
18. Wang H, Zhao T, Zhi L, Yan Y, Yu Y. Synthesis of novalac/layered silicate nanocomposites by reaction exfoliation using acid-modified montmorillonite. Macromol Rapid Commun. 2002;23:44–8.

19. Wang H, Zhao T, Yan Y, Yu Y. Synthesis of resol-layered silicate nanocomposites by reaction exfoliation with acid modified montmorillonite. J Appl Polym Sci. 2004;92:791–7.
20. Bahramian AR, Kokabi M. Ablation mechanism of polymer layered silicate nanocomposite heat shield. J Hazard Mater. 2009;166:445–54.
21. Manfredi LB, Puglia D, Kenny JM, Vázquez A. Structure-properties relationship in resol/montmorillonite nanocomposites. J Appl Polym Sci. 2007;104(5):3082–9.
22. Manfredi LB, Puglia D, Tomasucci A, Kenny JM, Vázquez A. Influence of the clay modification on the properties of resol nanocomposites. Macromol Mater Eng. 2008;293(11):878–86.
23. Rivero G, Vázquez A, Manfredi LB. Resol/montmorillonite nanocomposites obtained by in situ polymerization. J Appl Polym Sci. 2009;114:32–9.
24. Natali M, Monti M, Puglia D, Kenny JM, Torre L. Ablative properties of carbon black and MWNT/phenolic composites: a comparative study. Compos A. 2012;43:174–82.
25. Koo JH, Natali M, Tate J, Allcorn E. Polymer nanocomposites as ablative materials-a comprehensive review. Int J Energ Mater Chem Propuls. 2013;12(2):119–62.
26. Srikanth I, Daniel A, Kumar S, Padmavathi N, Singh V, Ghosal P, Kumar A, Rohini Devi G. Nano silica modified carbon–phenolic composites for enhanced ablation resistance. Scr Mater. 2010;63:200–3.
27. Ollier R, Vazquez A, Alvarez VA. Biodegradable nanocomposites based on modified bentonite and polycaprolactone. In: Advances in nanotechnology, vol. 10. New York: Nova Publishers; 2011.
28. Manfredi LB, de la Osa O, Galego Fernández N, Vázquez A. Structure-properties relationship for resols with different formaldehyde/phenol molar ratio. Polymer. 1999;40:3867–75.
29. Kissinger HE. Reaction kinetics in differential thermal analysis. Anal Chem. 1957;29(11):1702–6.
30. Vyazovkin S, Burnham AK, Criado JM, Pérez-Maqueda LA, Popescu C, Sbirrazzuoli N. ICTAC Kinetics Committee recommendations for performing kinetic computations on thermal analysis data. Thermochim Acta. 2011;520:1–19.
31. Brown ME, Maciejewski M, Vyazovkin S, Nomen R, Sempere J, Burnham A, Opfermann J, Strey R, Anderson HL, Kemmler A, Keuleers R, Janssens J, Desseyn HO, Li C-R, Tang TB, Roduit B, Malek J, Mitsuhashi T. Computational aspects of kinetic analysis: part A: the ICTAC kinetics project-data, methods and results. Thermochim Acta. 2000;355:125–43.
32. Friedman HL. Kinetics of thermal degradation of char-forming plastics from thermogravimetry. J Polym Sci Part C Polym Lett. 1964;6:183–95.
33. Akahira T, Sunose T. Joint convention of four electrical institutes. Res Rep Chiba Inst Technol. 1971;16:22–31.
34. Vyazovkin S, Sbirrazzuoli N. Isoconversional kinetic analysis of thermally stimulated processes in polymers. Macromol Rapid Commun. 2006;27:1515–32.
35. Lesnikovich AI, Levchik SV. A method of finding invariant values of kinetic parameters. J Therm Anal. 1983;27:89–94.
36. Ezquerro CZ, Ric GI, Miñana CC, Bermejo JS. Characterization of montmorillonites modified with organic divalent phosphonium cations. Appl Clay Sci. 2015;111:1–9.
37. Xi Y, Ding Z, He H, Frost RL. Structure of organoclays—an X-ray diffraction and thermogravimetric analysis study. J Colloid Interface Sci. 2004;277:116–20.
38. Xi Y, Frost RL, He H, Kloprogge T, Bostrom T. Modification of Wyoming montmorillonite surfaces using a cationic surfactant. Langmuir. 2005;21:8675–80.
39. Puglia D, Manfredi LB, Vazquez A, Kenny JM. Thermal degradation and fire resistance of epoxy–amine–phenolic blends. Polym Degrad Stab. 2001;73:521–7.
40. Lum R, Wilkins CW, Robbins M, Lyons AM. Thermal analysis of graphite and carbon-phenolic composites by pyrolysis-mass spectrometry. Carbon. 1983;21(2):111–6.
41. Puglia D, Kenny JM, Manfredi LB, Vázquez A. Influence of chemical composition on the thermal degradation and fire resistance of resol type phenolic resins. Mater Eng. 2001;12(1):55–72.
42. Ray SS, Okamoto M. Polymer/layered silicate nanocomposites: a review from preparation to processing. Prog Polym Sci. 2003;28(1):1539–641.
43. Surender R, Mahendran A, Thamaraichelvan A, Alam S, Vijayakumar CT. Model free kinetics—thermal degradation of bisphenol A based polybismaleimide–cloisite 15a nanocomposites. Thermochim Acta. 2013;562:11–21.
44. Pitchaimari G, Sarma KSS, Varshney L, Vijayakumar CT. Influence of the reactive diluent on electron beam curable funtionalized *N*-(4-hydroxyl phenyl) maleimide derivatives—studies on thermal degradation kinetics using model free approach. Thermochim Acta. 2014;597:8–18.
45. Goswami A, Srivastava G, Umarji AM, Madras G. Thermal degradation kinetics of poly(trimethylol propane triacrylate)/poly(hexane diol diacrylate) interpenetrating polymer network. Thermochim Acta. 2012;547:53–61.
46. Vyazovkin S, Wight CA. Kinetics in solids. Annu Rev Phys Chem. 1997;48:125–49.
47. Budrugeac P, Criado JM, Gotor FJ, Malek J, Perez-Maqueda LA, Segal E. On the evaluation of the nonisothermal kinetic parameters of $(GeS_2)(0.3)(Sb_2S_3)(0.7)$ crystallization using the IKP method. Int J Chem Kinet. 2004;36:309–15.
48. Vyazovkin S, Linert W. False isokinetic relationships found in the nonisothermal decomposition of solids. Chem Phys. 1995;193:109–18.
49. Perez-Maqueda LA, Criado JM, Gotor FJ, Malek J. Advantages of combined kinetic analysis of experimental data obtained under any heating profile. J Phys Chem A. 2002;106(12):2862–8.